

Mapping the conversion point in vertical transversely isotropic (VTI) media

Jianli Yang and Don. C. Lawton

ABSTRACT

The important aspect of converted-wave (P-S) seismology is that the exact location of P-S conversion point at the reflector is not well known. For a single horizontal layer, the position of the conversion point can be calculated exactly from an analytic expression. In multi-layered strata, the conversion point is not at a constant offset from the source, but traces a trajectory that moves towards the receiver as the depth decreases. The earth is known to be anisotropic, although basic seismic survey planning and data-processing are based on the isotropic assumption. The most common anisotropic case is Vertical Transversely Isotropic (VTI) media. In VTI media, there can be a large difference between the true coordinate of the conversion point and the one obtained from the isotropic single-layered model. This horizontal displacement of the conversion point in VTI media from that in the isotropic case is dependent on the offset-to-depth ratio, velocity ratio, and anisotropic parameters ϵ and δ defined by Thomsen. The relationship linking the displacement and the anisotropic parameters, and offset-to-depth ratio, can be complicated. An algorithm to calculate this relationship is developed using Thomsen's anisotropy equations, both the linear approximation and the exact forms. A VTI model is designed using NORSAR2D software and the common-shot raytracing is performed to obtain the conversion-point coordinate. The displacement of the conversion point increases with the increasing offset to depth ratio and the anisotropy parameter ϵ . The value of δ can also have large influence on the displacement of the conversion point. We conclude that when the anisotropic parameter ϵ is smaller than δ , the conversion point is displaced towards the receiver relative to its location in an isotropic medium. When ϵ is larger than δ , the conversion point moves towards the source compared to that in the isotropic medium. There is no large difference between the results from Thomsen's linear equations and the results from exact equations at small offset-to-depth ratios.

INTRODUCTION

Converted waves have been more and more widely used in seismic exploration, for they can provide high-quality images where conventional images are poor (Stewart et al., 1999). Figure 1 shows the geometry of the converted wave in a thick, uniform isotropic layer.

A ray emitted as a P-wave at angle θ_p from the source reflects from the bottom of the layer as an S-wave at an angle θ_s and is received at the receiver at a certain offset. These two angles are related by Snell's law:

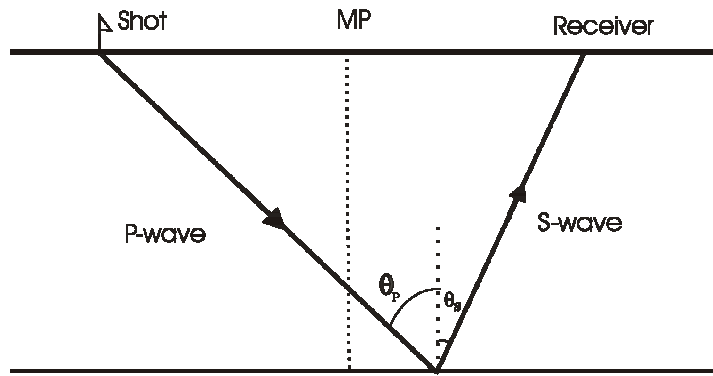


FIG. 1. The geometry of the converted wave obeying Snell's law.

$$\frac{\sin \theta_p}{v_p} = \frac{\sin \theta_s}{v_s} = p \tag{1}$$

Here p is the ray parameter, and v_p is the P- wave velocity and v_s is the S-wave velocity.

The distance of the conversion point from the source is dependent on the depth of the reflector and the v_p/v_s in the overburden. Tessmer and Behle (1988) gave a formula to calculate approximately the coordinate of the conversion point in an homogeneous and isotropic layer, which for a small incident angle is:

$$x_{pa} = \frac{x}{1 + \left(\frac{v_s}{v_p} \right)} \tag{2}$$

Because the P-S velocity ratio v_p/v_s is always larger than 1, the conversion point is closer to the receiver than the midpoint. The S-wave leg comes up more steeply than the P-wave leg goes down. They concluded that for deeper reflection zones the approximation errors are small.

Tessmer and Behle (1988) showed that in multi-layered strata, the conversion point is not a constant offset from the source, but traces a trajectory that moves towards the receiver as the depth decreases (Figure 2). The asymptote of this trajectory is defined by equation (2). A multi-layered model can be considered as a simple case of VTI medium.

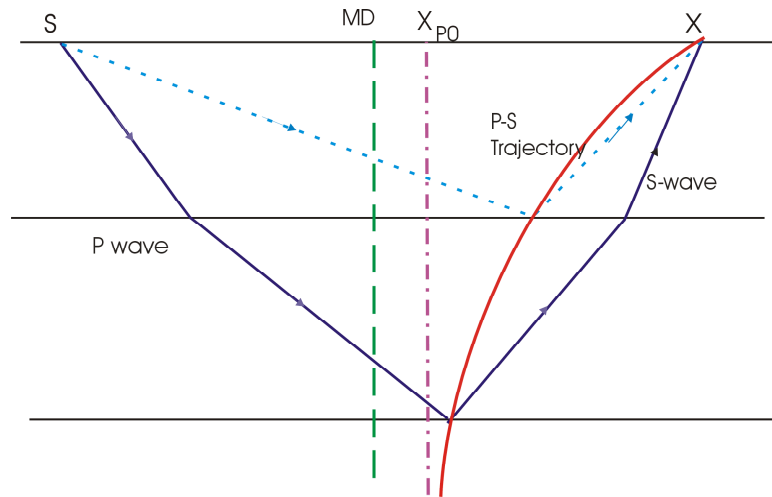


FIG. 2. The conversion point traces a trajectory in the multi-layered model for a certain offset, instead of locating on a vertical axis (Stewart et al., 1999).

It's well known that the earth's crust is inhomogeneous and anisotropic. But almost all of the seismic surveys and processing have not taken anisotropy into consideration. This isotropy assumption could lead to large errors in NMO correction, stacking and migration, which have been shown by many authors (e.g. Alkhalifah and Lerner, 1994). The most commonly considered anisotropic medium is the Vertical Transversely Isotropic (VTI) case. Thomsen (1986) showed that the energy does not travel along the direction that the ray path travels in the anisotropic case because the wavefront is not spherical (Figure 3).

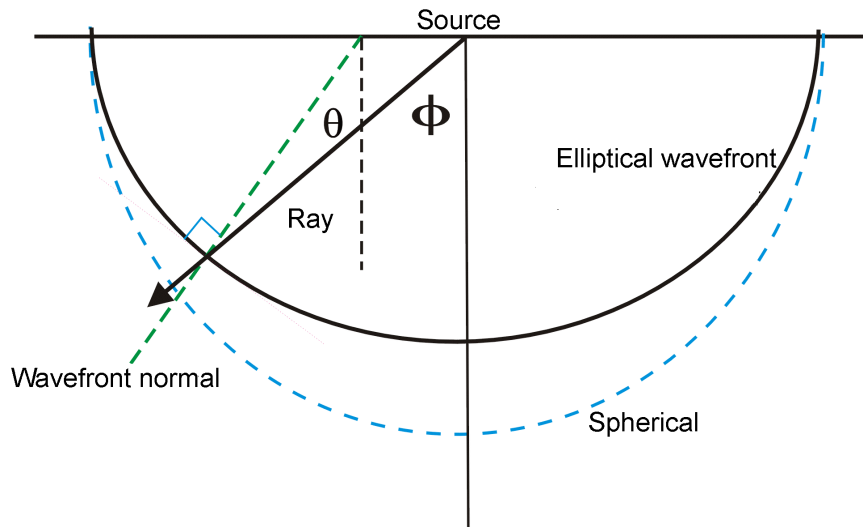


FIG. 3. Graph of the definitions of phase (wavefront) angle, θ , and group (ray) angle, ϕ (Thomsen, 1986).

The wavefront-normal angle is called the ray angle, which is represented as θ while the angle from the source point to the wavefront is called the phase angle, which is represented by ϕ . The phase velocity (velocity perpendicular to the wavefront) is

different from the group velocity. Thomsen (1986) showed the difference between the ray angle and the phase angle in an anisotropic case in Figure 3. He defined three parameters ε , δ and γ to describe these different varieties of anisotropy. He also deduced the velocity equations, which are functions of the phase angle and the anisotropic parameters, and the relationship between the phase angle and the group angle.

Anisotropy has less influence on P-waves than on S-(converted) waves. When the formation is shown to be VTI, the location of the conversion point will depart horizontally from that in an isotropic case, and it cannot be approximated by the isotropic case. Otherwise, it will lead to great problems in NMO correction and stacking which could cause traces that do not contain reflector energy to be summed, and those that do contain reflector energy not to be summed (Tessmer et al., 1990). Lawton and Cary (2000) proved that the location of the conversion point is critical to the P-S seismic survey design. Therefore, the horizontal position of the conversion point on the reflector has to be calculated specifically. In this paper we concentrate on the calculation of the displacement of the conversion point in the VTI model.

THEORY

Starting from the linear stress-strain equations, Thomsen (1986) gave his definition of the anisotropy parameters connected with the velocities rather than the elastic components. He used ε to describe the fractional difference between vertical and horizontal P velocities, which is given by

$$\varepsilon = \frac{v(\pi/2) - \alpha_0}{\alpha_0} \quad (3)$$

The parameter δ , is defined to describe the near-vertical P-wave propagation by

$$\delta = 4 \left[\frac{V_p(\pi/4)}{V_p(0)} - 1 \right] - \left[\frac{V_p(\pi/2)}{V_p(0)} - 1 \right] \quad (4)$$

And also γ , which corresponds to the conventional meaning of “SH anisotropy” is expressed by

$$\gamma = \frac{v_{sh}(\pi/2) - \beta_0}{\beta_0} \quad (5)$$

He obtained the equations of phase velocity in transversely isotropic media:

$$v_p^2(\theta) = \alpha_0^2 [1 + \varepsilon \sin^2 \theta + D^*(\theta)] \quad (6)$$

$$v_{sv}^2(\theta) = \beta_0^2 \left[1 + \frac{\alpha_0^2}{\beta_0^2} \varepsilon \sin^2 \theta - \frac{\alpha_0^2}{\beta_0^2} D^*(\theta) \right] \quad (7)$$

$$v_{SH}^2(\theta) = \beta_0^2 [1 + 2\gamma \sin^2 \theta] \quad (8)$$

with

$$D^*(\theta) = \frac{1}{2} \left(1 - \frac{\alpha_0^2}{\beta_0^2} \right) \left\{ \left[1 + \frac{4\delta^*}{(1 - \beta_0^2/\alpha_0^2)} \sin^2 \theta \cos^2 \theta + \frac{4(1 - \beta_0^2/\alpha_0^2 + \varepsilon)\varepsilon}{(1 - \beta_0^2/\alpha_0^2)} \sin^4 \theta \right]^{\frac{1}{2}} - 1 \right\} \quad (9)$$

where α_0, β_0 is the P-wave phase velocity and S-wave velocity in the vertical axis, respectively. And they are defined by

$$\alpha_0 = \sqrt{\frac{(k + 4\mu/3)}{\rho}} \quad (10)$$

$$\beta_0 = \sqrt{\frac{\mu}{\rho}} \quad (11)$$

Here, k is bulk modulus and μ is the shear modulus and ρ is density.

The ray angle, ϕ , can be expressed as a function of phase angle, θ , given by the following equation:

$$\tan[\phi(\theta)] = \frac{(\tan\theta + \frac{1}{v} \frac{dv}{d\theta})}{(1 - \frac{\tan\theta}{v} \frac{dv}{d\theta})} \quad (12)$$

Group velocity at angle ϕ , $V(\phi)$, is related to phase velocities at angle θ by:

$$V^2[\phi(\theta)] = v^2(\theta) + \left(\frac{dv}{d\theta} \right)^2 \quad (13)$$

Using the Taylor-series expansion for small ε , δ^* and γ , Thomsen derived the linear approximation for weak anisotropy:

$$D^*(\theta) \approx \frac{\delta^*}{\left(1 - \beta_0^2/\alpha_0^2 \right)} \sin^2 \theta \cos^2 \theta + \varepsilon \sin^4 \theta \quad (14)$$

So substituting the equation (14) into the equations (6), (7) and (8), respectively, he obtained the following linear approximation of the velocities:

$$v_p(\theta) = \alpha_0(1 + \delta \sin^2 \theta \cos^2 \theta + \varepsilon \sin^4 \theta) \quad (15)$$

$$v_{sv}(\theta) = \beta_0 \left(1 + \frac{\alpha_0^2}{\beta_0^2} (\varepsilon - \delta) \sin^2 \theta \cos^2 \theta \right) \quad (16)$$

$$v_{sh}(\theta) = \beta_0(1 + \gamma \sin^2 \theta) \quad (17)$$

Thomsen (1986) then replaced the δ^* with another parameter, δ , using the relationship:

$$\delta = \frac{1}{2} \left[\varepsilon + \frac{\delta^*}{(1 - \beta_0^2/\alpha_0^2)} \right] \quad (18)$$

The relationship between the group angle, ϕ , and phase angle, θ , in the linear approximation form, is:

$$\tan \phi = \tan \theta \left[1 + \frac{1}{\sin \theta \cos \theta} \frac{1}{v(\theta)} \frac{dv}{d\theta} \right] \quad (19)$$

For P waves, substituting equation (15) into equation (12) leads to

$$\tan \phi_p = \tan \theta_p \left[1 + 2\delta + 4(\varepsilon - \delta) \sin^2 \theta_p \right] \quad (20)$$

Similarly, for SV-wave and SH-wave,

$$\tan \phi_{sv} = \tan \theta_{sv} \left[1 + 2 \frac{\alpha_0^2}{\beta_0^2} (\varepsilon - \delta) (1 - 2 \sin^2 \theta_{sv}) \right] \quad (21)$$

$$\tan \phi_{sh} = \tan \theta_{sh} (1 + 2\gamma) \quad (22)$$

These equations are the theoretical bases for the calculation of the horizontal coordinate of the conversion point for given offset/depth ratio, and anisotropy parameters.

NUMERICAL MODELLING METHODOLOGY AND RESULTS

Mapping conversion point using Thomsen's equation

Using Thomsen's linear-approximation equations (equations (16)-(21)), we develop an algorithm to calculate the horizontal distance between the theoretical conversion points in a VTI medium and in an isotropic medium for the same offset. We follow the same procedure using the same equations (equations (6), (7), (8), and 12), as described in the following paragraphs. Figure 4 shows the flow of this algorithm developed to calculate the displacement of the conversion point.

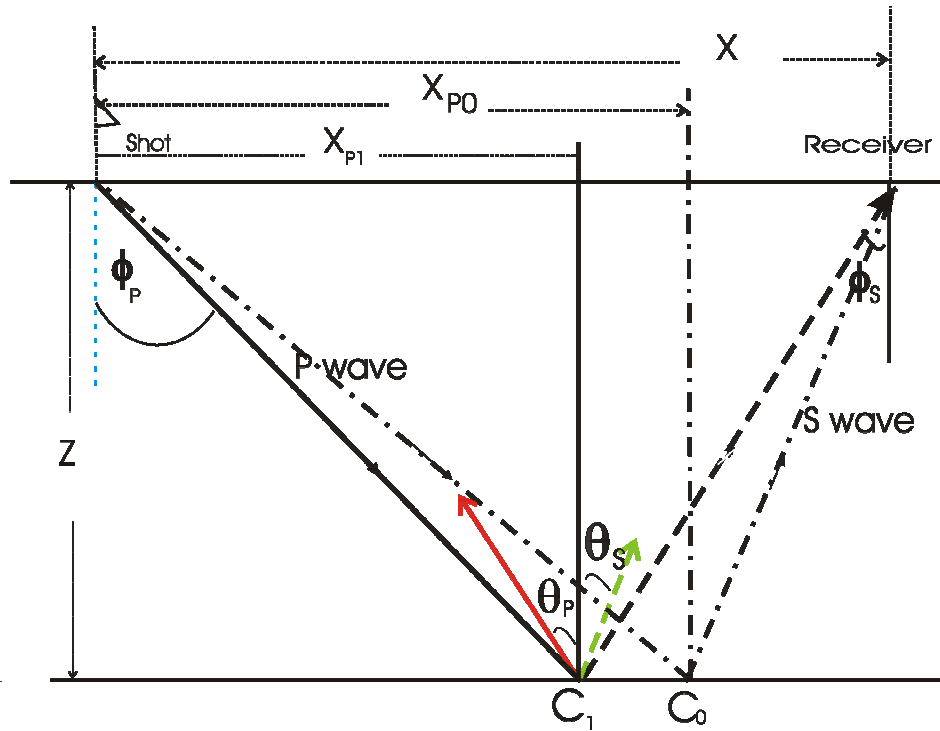


FIG. 4. Chart showing the angles and offsets included in the algorithm.

The basic method computes P-wave phase angles θ_p (such as from 0 to 60 degrees, with a step of 0.25 degrees), then the corresponding P-wave phase velocity at each angle, $v_p(\theta)$, is calculated by using equation (6), and then the P-wave ray parameter, p_p , for each angle by using equation (1).

A series of SV-wave phase velocity, $v_s(\theta)$, are calculated using equation (7) for a number of SV wave reflection angle (such as from 0 to 60 degrees, with interval of 0.25 degree), then the SV-wave ray parameter p_s .

For each P-wave ray parameter, the SV-wave ray parameter that is equal or the closest to it is found and the corresponding values of the SV-phase angle stored.

For each P-wave phase angle, and for given values of ϵ and δ , the group angle, ϕ_p , is first calculated using Thomsen's exact equation (12). The horizontal coordinate of the conversion point X_{p1} is calculated by using the group angle and the thickness of the VTI medium in the formula $X_{p1} = z * \tan \phi_p$.

For each S-wave phase angle that has been stored, which corresponds to each P-wave phase angle by Snell's law, its group angle ϕ_s is calculated by using equation (12). Then the distance from the conversion point to the receiver X_{s1} , shown in Figure 4, is calculated from $X_{s1} = z * \tan \phi_{sv}$, which is the distance between the conversion point and the receiver.

A series of offsets X for each phase angle θ_p can be obtained by adding these two distances together: the distance from the conversion point to the source X_{p1} , and the distance from the conversion point to the receiver X_{s1} . Also the corresponding offset-to-depth ratio can be obtained.

Then given the offset X in a VTI medium, the conversion-point offset for this shot–receiver offset, X_{p0} , can be determined using the same P-wave velocity and S-wave velocity by Snell's law for different angles. The distance between the two conversion points ($X_{p0} - X_{p1}$), which is the displacement of the conversion point in VTI media from that in isotropic case for same offset, is then obtained.

The linear approximation forms of ray angle (equations (20), (21), and (22)) and phase velocities (equations (15), (16) and (17)), can also be applied replacing the exact equations.

For the model with $\varepsilon = 0.10$, and $\delta = 0.05$, the displacement of the conversion point, relative to the isotropic case is calculated using Thomsen's exact equations for phase velocities and ray angles and linear-approximation equations, respectively. The same procedures are conducted for $\delta = 0.10$ and $\delta = 0.2$. Figure 5.1 and Figure 5.2 display the variation of the displacement with the variation of the offset to depth ratio. From these two figures we can see there is no significant difference between these two methods.

A series of 3-D curved surfaces are also plotted to display the variation of the displacement of the conversion point and the offset-to-depth ratio, and the anisotropy parameter ε (Figure 6.1-6.6), which are obtained from the exact equation of energy velocities and ray angles (equations (6), (7), (8) and (12)).

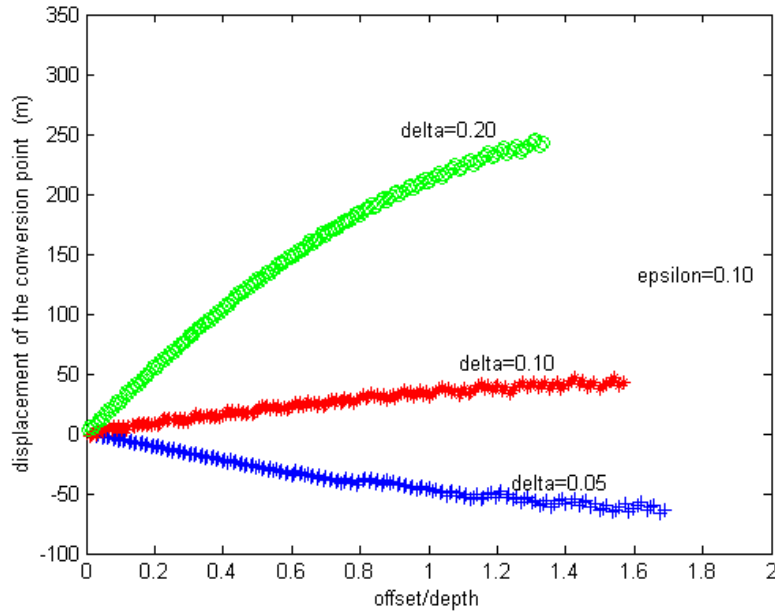


FIG. 5.1 Variation of the displacement of the conversion point with the variation of the offset to depth ratio, computed from Thomsen's linear approximation of phase velocities equation (equations (15), (16) and (17)) and ray angle (equations (20), (21) and (22)) for different value of delta. In this figure, the '+' sign represents the conversion point moves towards receiver, while '-' represents the conversion point moves towards to the source, relative to that in isotropic case.

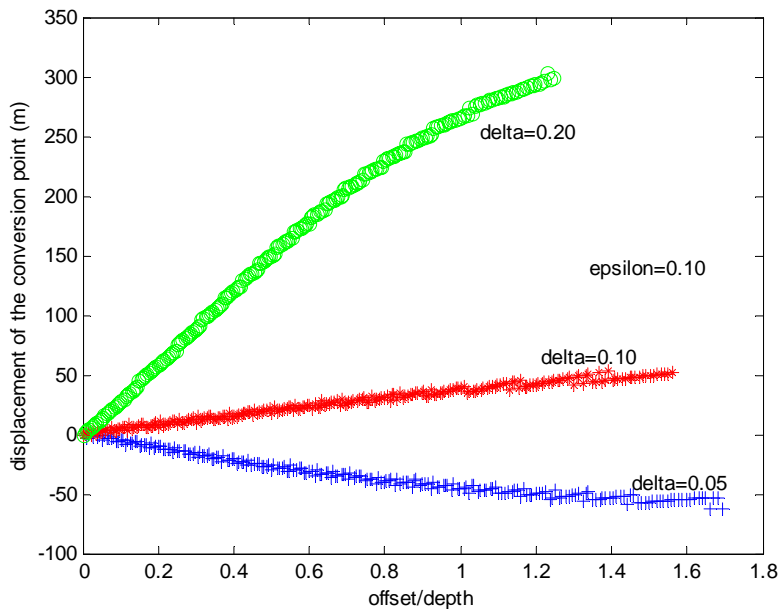


FIG. 5.2 Variation of the displacement of the conversion point with the variation of the offset to depth ratio, computed from Thomsen's exact equations for phase velocities equation (equations (6),(7) and (8)), and ray angle(equation (12)).

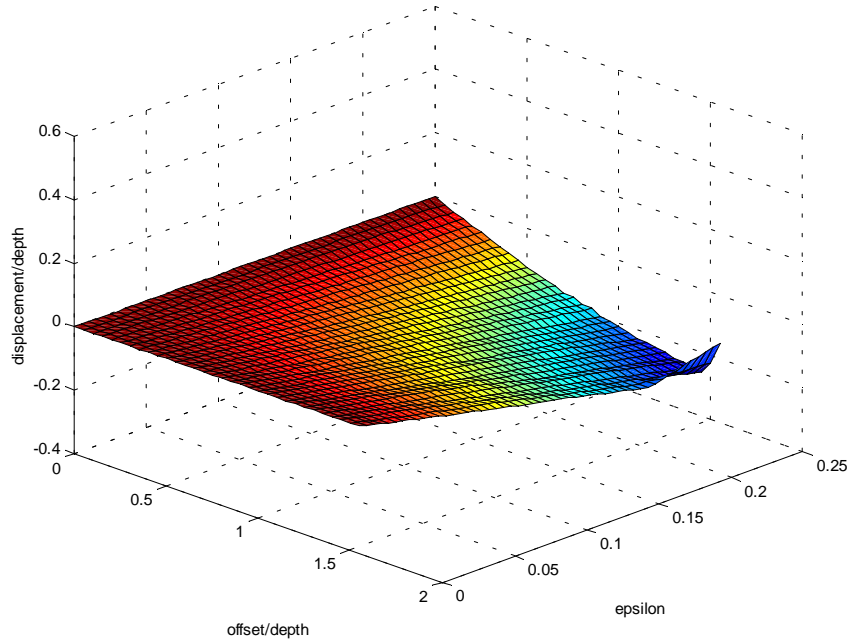


FIG. 6.1 3-D surface showing the variation of the displacement-to-depth ratio of the conversion point in VTI media relative to its location in the isotropic case, with the variation of the offset-to-depth ratio and ϵ . Here, $\delta = 0.25 \epsilon$.

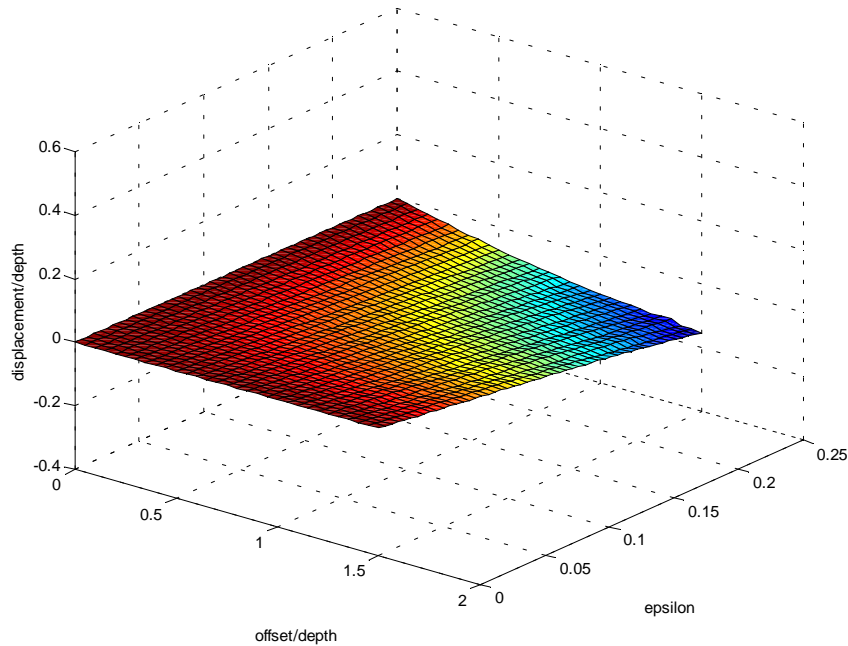


FIG. 6.2 3-D surface showing the variation of the displacement-to-depth ratio of the conversion point in VTI media relative to its location in the isotropic case, with the variation of the offset-to-depth ratio and ϵ . Here, $\delta = 0.50 \epsilon$.

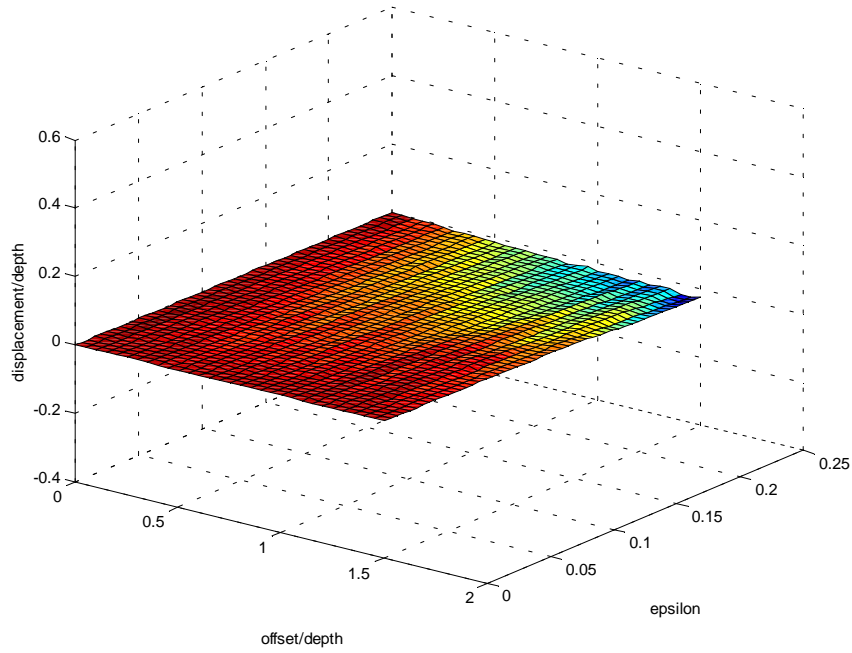


FIG. 6.3 3-D surface showing the variation of the displacement-to-depth ratio of the conversion point in VTI media relative to its location in the isotropic case, with the variation of the offset-to-depth ratio and ϵ . Here, $\delta = 0.75 \epsilon$.

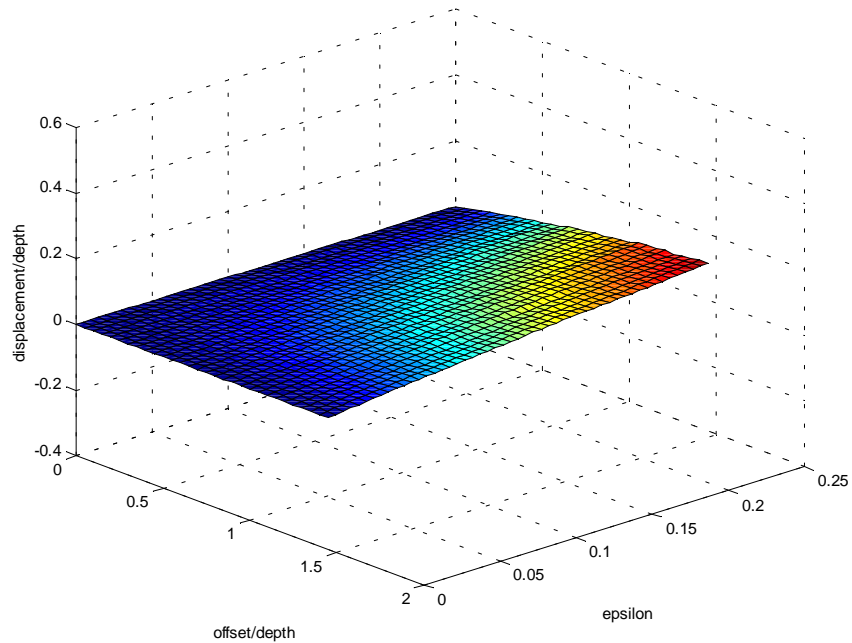


FIG. 6.4 3-D surface showing the variation of the displacement-to-depth ratio of the conversion point in VTI media relative to its location in the isotropic case, with the variation of the offset-to-depth ratio and ϵ . Here, $\delta = 1.0 \epsilon$.

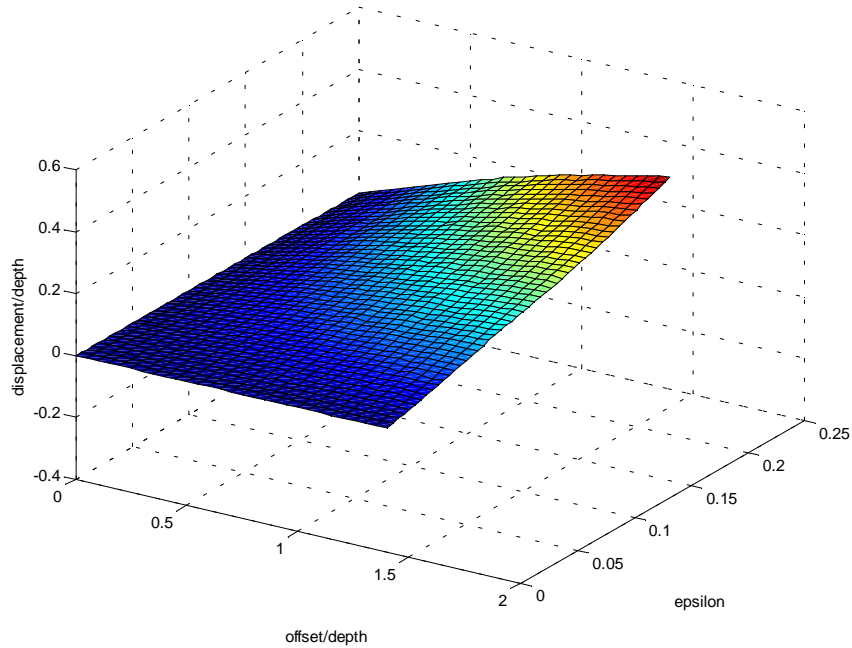


FIG. 6.5 3-D surface showing the variation of the displacement-to-depth ratio of the conversion point in VTI media relative to its location in the isotropic case, with the variation of the offset-to-depth ratio and ϵ . Here, $\delta = 1.25 \epsilon$.

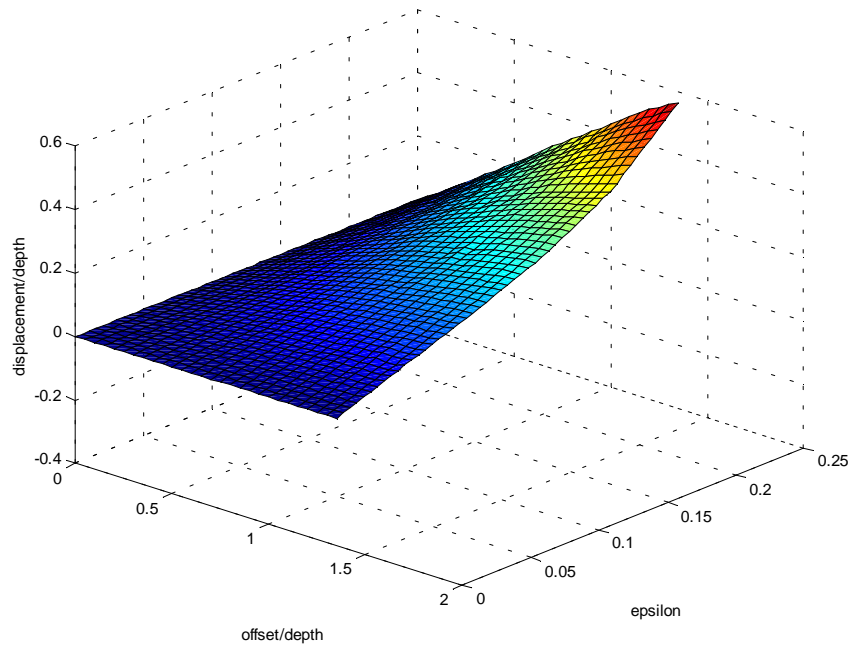


FIG. 6.6 3-D surface showing the variation of the displacement-to-depth ratio of the conversion point in VTI media relative to its location in the isotropic case, with the variation of the offset-to-depth ratio and ϵ . Here, $\delta = 1.5 \epsilon$.

NORSAR 2D anisotropy ray mapping

A VTI model (Figure 7) is designed and anisotropic ray-mapping is conducted by using the NORSAR2D package to get the displacement of conversion point.

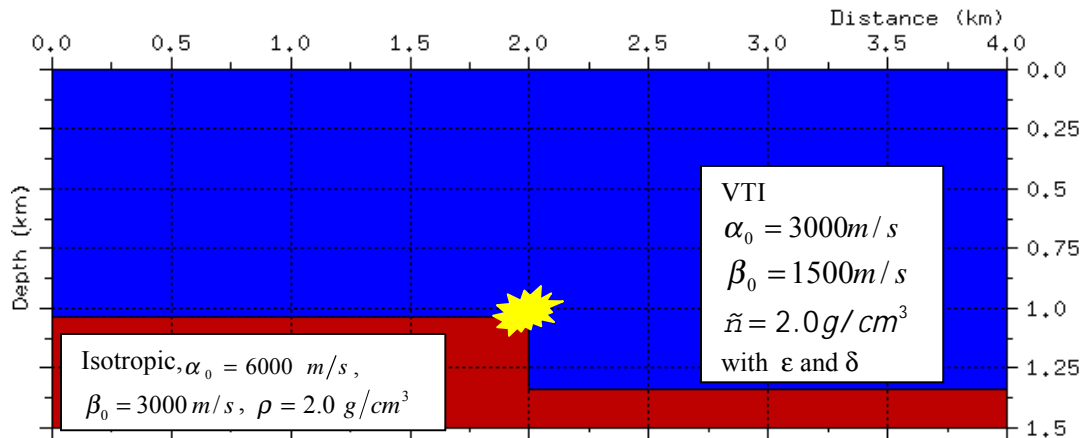


FIG. 7. The geometry and physical properties of the VTI model designed for NORSAR2D.

The physical parameters ($\alpha_0, \beta_0, \rho, \epsilon, \delta, \gamma$) and the size of the model we designed are kept constant as they were defined in our algorithm. A special point ($x = 2.0 \text{ km}$, $z = 1.036 \text{ km}$), which is marked with a star, is used to detect the trace number conveniently.

The common-shot survey, with P-wave vertical source and horizontal S-wave receiver, is conducted in the raytracing on this model.

The synthetic seismograms are generated by the NORSAR2D and displayed by PROMAX. In every case the event is broken at the special point (conversion point) on the synthetic seismogram. Displaying this seismogram on PROMAX, we know the trace number, so we can determine the offset. An example of the synthetic seismogram is shown in Figure 8.

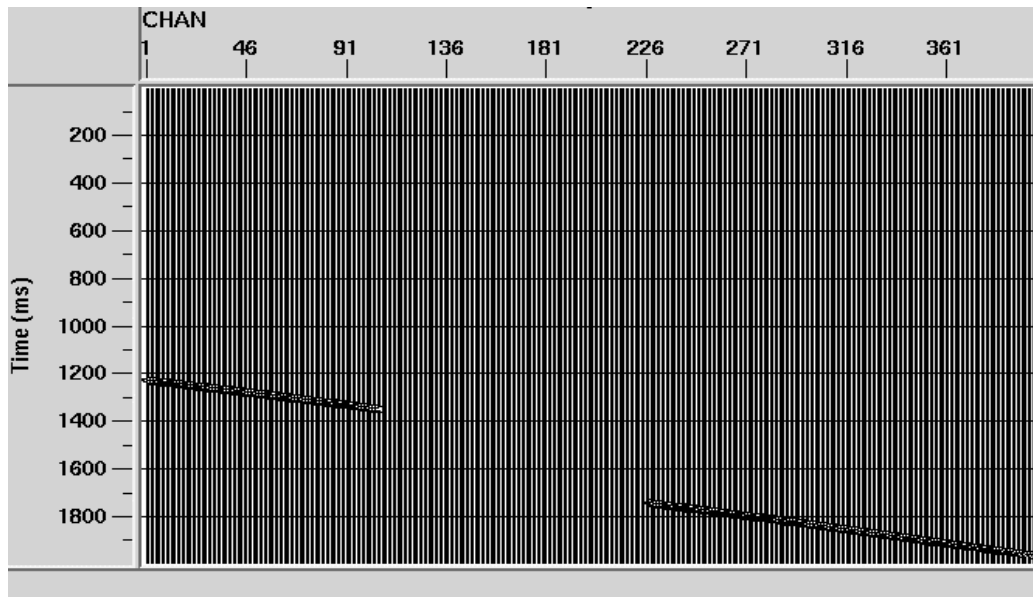


FIG. 8. An example of P-S wave synthetic seismogram, is generated from NORSAR2D and displayed in PROMAX.

The horizontal coordinate of the conversion point X_{p1} for a certain offset-to-depth ratio is obtained from the display of the synthetic seismogram. The offset of conversion point in the isotropic case, X_{po} , is also obtained by performing the common-shot raytracing. The displacement of the conversion point can be obtained by calculating $X_{p1} - X_{po}$.

The results obtained by using NORSAR2D are shown in Table 1 and Table 2, for $\epsilon = 0.10$ and $\epsilon = 0.20$, respectively. For comparison with the results from our algorithm, the corresponding displacement obtained from the Thomsen's exact equations and linear approximations are also listed together.

Table 1. Comparison of the conversion point's displacement in the VTI model relative to its location in the isotropic case, obtained from NORSAR2D raytracing with that calculated using Thomsen's linear approximations and exact equations. The offset-to-depth ratio is 1.34 and $\epsilon = 0.10$. The '+' sign means the conversion point moves towards the receiver, and '-' towards the shot.

For $\epsilon = 0.10$	Displacement from NORSAR2D (m)	Displacement from linear equations (m)	Displacement from exact equations (m)
$\delta = 0.20$	236.1	244.18	316.42
$\delta = 0.15$	142.3	139.16	163.58
$\delta = 0.10$	47	41.56	49.53
$\delta = 0.05$	-50	-56.50	-49.39
$\delta = 0.00$	-146	-151.26	-140.15
$\delta = -0.05$	-244	-237	-218.68

Table 2. Comparison of the conversion-point's displacement in the VTI model relative to its location in the isotropic case, obtained from NORSAR2D raytracing with that calculated using Thomsen's linear approximations and exact equations. The offset-to-depth ratio is 1.34 and $\epsilon = 0.20$. The '+' sign means the conversion point moves towards the receiver, and '-' towards the shot.

For $\epsilon = 0.20$	Displacement from NORSAR2D (m)	Displacement from linear equations (m)	Displacement from exact equations (m)
$\delta = 0.30$	255	267.69	383.69
$\delta = 0.20$	82	73.70	83.43
$\delta = 0.15$	-4	-18.49	-13.73
$\delta = 0.10$	-171	-103.70	-100.17
$\delta = 0.05$	-180	-189.26	-177.24

From Table 1 and Table 2, we can see that the results from different methods show the same variation trend. The conversion point in VTI media moves towards the receiver when $\epsilon \leq \delta$ and towards the shot while $\epsilon > \delta$. The displacements from the NORSAR2D experiments are much closer to the results from Thomsen's linear equations than to the results from the exact equations.

The raypath of the P-S wave in the VTI model with $\epsilon = 0.10$, $\delta = -0.05$ and $\delta = 0.20$, respectively, and the raypath in isotropic case, are also plotted to show the displacement of the conversion point (Figure 10). In this case, the distance of these two conversion points in the VTI model with different values of δ can be as large as 480, which may due to the influence of the value of δ .

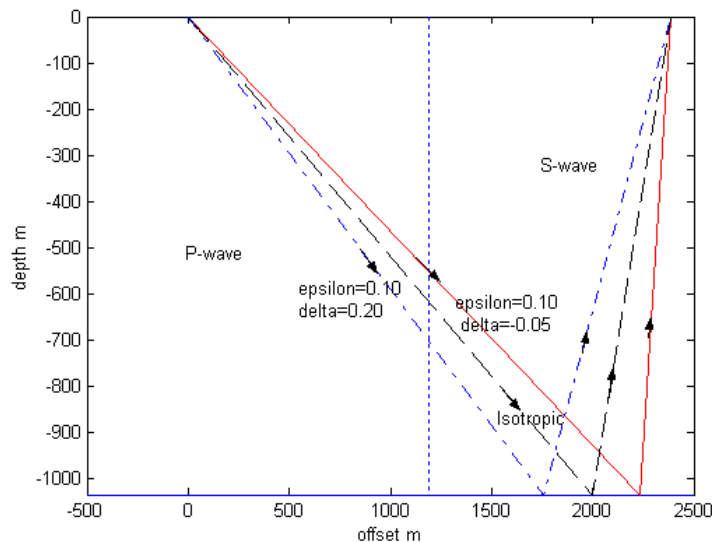


FIG. 9. The displacement of the conversion point in VTI model with $\epsilon = 0.10$, $\delta = -0.05$ and $\delta = 0.20$, respectively.

DISCUSSION AND CONCLUSION

Results from the analysis show that the conversion point in the anisotropic case is very different from that in the isotropic case. The horizontal displacement of the conversion point in VTI media from that in isotropic media is dependent on the velocity ratio, offset-to-depth ratio, and anisotropy parameters (Figures 6.1-6.6). It increases with the increasing offset-to-depth ratio and anisotropic parameter ϵ (Figures 6.1-6.6).

When ϵ is larger than δ , for the same offset, the conversion point moves towards the source in VTI media relative to that in the isotropic case (Figures 6.1-6.3, and Figures 5.1-5.2). When ϵ is smaller than or equal to δ for same offset, the conversion point moves towards the receiver (Figures 6.4-6.6, and Figures 5.1-5.2). Before this experiment was conducted, it had been assumed generally that the conversion point moves towards the source with increasing anisotropy.

It has been proven that in most sedimentary formations, the value of ϵ is larger than the value of δ (Thomsen, 1986). So, the conversion point moves towards the source in most cases of VTI media. The displacement of the conversion point cannot be ignored in formations with transversely isotropic characteristics, which would cause a large error if anisotropy is not taken into account (Figures 6.1-6.6). When the formation is shown to be anisotropic, the conversion point can't be approximated by the position found in the isotropic case.

There is no significant difference between the results obtained from Thomsen's exact equations for anisotropic velocities and ray-angle calculations (equations (6), (7), (8), and (12)), and the results from the linear-approximation equations (equations (15), (16), (17), and (20), (21), (22)), for small offset-to-depth ratios, but there is a large difference for offset-to-depth ratios greater than 1.5. (Figure 5.1 and Figure 5.2)

The result from the NORSAR2D software is close to our results obtained from Thomsen's linear equations for weak anisotropy (Table 1 and Table 2). It has been shown that the value of δ can also have a significant influence on the location of the conversion point.

All our calculations are based on the assumption that the accuracy of measurement of the anisotropy parameters can be guaranteed.

ACKNOWLEDGEMENTS

The authors thank CREWES for providing the necessary software needed to conduct this project. We also thank Dr. Larry Lines and Dr. Jim R. Brown of CREWES for valuable suggestions. The financial support of CREWES sponsors is also greatly appreciated.

REFERENCES

- Lawton, D.C., and Cary W. P., 2000, Conversion point mapping and interpolation in P-S survey design, CREWES Annual Research Report, Volume 12, 53-62
- Lawton, D.C., Hoffe, B., and Cary W.P., 2000, Some design issues for 3D P-S seismic survey, SEG/EAGE Summer Research Workshop
- Stewart, R.R., Gaiser, J.E., Brown, R.J., and Lawton, D.C., 1999, Converted-wave seismic exploration: a tutorial, CREWES Annual Research Report, Volume 11, 21-62
- Tessmer, G., and Behle, A., 1988, Common reflection point data-stacking technique for converted waves, Geophysical Prospecting, Volume 36, 671-688
- Tessmer, G., Krajewski, P., Fertig, J., and Behle, A., 1990, Processing of PS reflection data applying common conversion-point stacking technique, Geophysical Prospecting, Volume 38, 267-286
- Thomsen, L., 1986, Weak elastic anisotropy: Geophysics, Vol.51, No.10, 1954-1966
- Thomsen, L., 1999, Converted-wave reflection seismology over inhomogeneous, anisotropic media: Geophysics, 64, 678-690.